Article

Incorporation of Torsion Springs in a Knee Exoskeleton for Stance Phase Correction of Crouch Gait

Katy B. Bumbard [1], Harold Herrington [1], Chung-Hyun Goh [1,*] and Alwathiqbellah Ibrahim [1]

[1] Department of Mechanical Engineering, The University of Texas at Tyler, Tyler, TX, 75799, USA.

* Correspondence: cgoh@uttyler.edu; Tel. 1-903-566-6125.

Abstract: Crouch gait is a motor complication commonly associated with cerebral palsy, spastic diplegia, stroke, and motor-neurological pathologies, broadly defined as knee flexion in excess of 20° in the gait cycle. Uncorrected crouch gait results in fatigue, joint degradation, and loss of ambulation. Torsion springs have been used in cycling to store energy in knee flexion to reduce fatigue in the quadriceps during knee extension. SolidWorks was used to design a passive exoskeleton for the knee, incorporating torsion springs of stiffnesses 20,000 N/mm and 30,000 N/mm at the knee joint to correct four different crouch gaits. OpenSim was used to gather data from moments produced and knee angles from each crouch gait and the normal gait. Motion analysis of the exoskeleton was simulated using knee angles for each crouch gait and compared with moments produced with the normal gait moments in the stance phase of the gait cycle. All crouch gait moments were significantly reduced, and the correction of peak crouch moments was achieved corresponding to the normal gait cycle during the stance phase. These results offer significant potential for nonsurgical and less invasive options for wearable exoskeletons in crouch gait correction.

Keywords: crouch gait; torsion springs; knee exoskeleton; stance phase; gait rehabilitation

1. Introduction

Crouch gait is defined as flexion in excess of 20° during the stance phase of the gait cycle [1,2]. Crouch gait is common in those with severe diplegia or spastic quadriplegia caused by conditions such as cerebral palsy (CP), stroke, multiple sclerosis (MS) and other neurological disorders. Causes of couch gait include contracted hamstrings, contracted hip flexors, impaired balance, foot deformities, impaired proprioception, and muscle weakness [3,4]. In addition, excessive flexion occurs during the stance phase of the gait cycle, resulting in degradation of joints, pain, and loss of ambulation over time [4,5,6].

There are two major phases of the normal gait cycle: the stance phase and the swing phase. The stance phase is the point of heel strike to toe-off, which occurs from 0% to 60% of the gait cycle [7]. The swing phase is defined as the point from toe-off from the previous phase at 60% of the gait cycle to the follow up heel strike at 100% of the gait cycle. Figure 1 describes the normal knee angle throughout one complete gait cycle for the right knee, where normal knee angles provided by OpenSim 4.3 were plotted with respect to the proportion of the gait cycle.
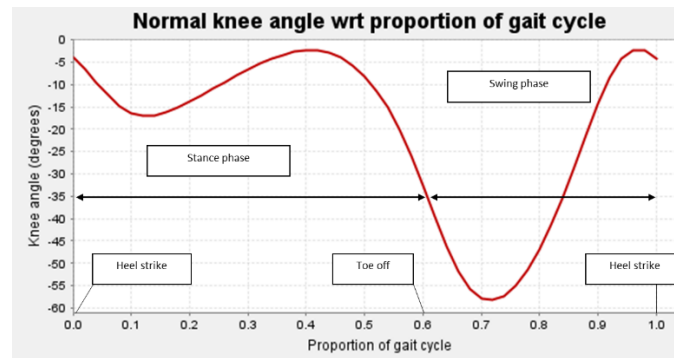
Figure 1. Normal knee angle by phase of gait cycle with respect to proportion of gait cycle .

Figure 1 shows as a proportion of the gait cycle for purposes of understanding knee flexion during each phase of the gait cycle.   The knee angle for the normal gait cycle (red) is compared to four different crouch gaits. Normal rotation of the knee ranges between -2.27° and -58.25°. For each crouch gait, the joint rotation has a severe limitation in range of motion. As a result, the knee cannot overcome extreme flexion during the stance phase of the gait cycle, which ends at about 60% of the gait cycle.

The knee extension and flexion are generated by force actuation in the quadriceps and hamstrings. Ganjwala et. al. notes that an imbalance in these results in deviation of gait resulting in flexed knee gait (FKG) or crouch gait, wherein excessive flexion occurs during the stance phase of the gait cycle [5]. Acceleration of the gluteus maximus and vasti are responsible for knee extension, thus lower velocities inhibit knee extension [8]. Causes of FKG include hamstring shortening, fixed flexion deformity of the knee, quadriceps weakness, patella tendon lengthening and soleus weakness. Due to the quadriceps having to work constantly to stabilize the knee, as opposed to short duration during a normal gait, FKG causes high energy consumption resulting in fatigue. Inefficiency in gait is well documented [9-12]. Complications of uncorrected crouch gait result in increases the load on the knee joint [13,2] which likely causes knee pain [5,14,15]and joint deterioration [2,16,17].

The stance phase of the gait cycle is the weightbearing portion of the gait cycle. When the foot maintains contact with the ground, the weight bearing axis should align centrally from the ankle and the knee [18], to the hip. In crouch gait, the weightbearing axis shifts to the posterior of the knee [19]. Tibiofemoral forces corresponding with ground reaction force peaks in the stance phase of the gait cycle are more than double [13] in crouch gait compared to unimpaired gait, depending on the severity of the crouch gait [2]. In crouch gait, Steele et.al. attributed the increasing Tibiofemoral force to increased force in the quadriceps throughout the stance phase. Additionally, crouch gait severity results in increased patellofemoral contact pressures as well as location [13] of patellofemoral contact pressure. Li et. al discussed altered tibiofemoral kinematics and resulting increased posterior translation of the tibia with increasing flexion and the correlation to knee pathology with increasing patellofemoral contact pressures [20] and hypothesized that balancing hamstrings and quadriceps forces could reduce patellofemoral contact pressure.

In many cases crouch gait is a result of torsional deformities [17,21] which tends to cause either an inward or outward position of the feet and ankles. Often rigid ankle-foot orthoses (AFOs) are used to aid in rehabilitation of people affected by gait deviation. Bregman et. al. studied the effects of using torsional springs in the ankles in stroke and multiple sclerosis patients [22] to achieve an energy efficient gait. Some AFOs incorporating torsion springs in the ankles show improvement of moments and flexion in the knee, however these did not improve knee angles to normal values [23].

Robotic or powered exoskeletons have the potential to improve gait movement and the overflexion of the knee [4]. Lerner et al. described the benefit a motorized version of a

lower-extremity assistance device, through strengthening the knee extensors and improving posture during the gait cycle that encouraged broader participation of the knee extensors throughout the stance phase of the normal gait cycle. While strength training of the knee extensors [24], especially in those with hamstring length within range for normal walking has potential for gait improvement, motorized assistive devices throughout the gait cycle provide for more optimum improvement in these muscle functions [4].

The majority of noninvasive, nonsurgical correction is through motorized lower limb exoskeletons that reduce the overall flexion of the knee in the stance phase of gait, while encouraging larger range of motion. The objective of this project is to develop a lower limb exoskeleton for rehabilitative purposes and perform a comparative dynamic analysis on the functionality of the exoskeleton with applied forces and torques as a result of several crouch gaits. We seek to develop a passive model rather than a motorized exoskeleton, using torsional springs, to off-load excessive forces [25] generated during the stance phase of gait. While research indicates the majority of complications occur at the ankle, and ideally an entire lower limb exoskeleton would be preferential, the objective is to analyze the results of offloading forces in a small portion of the leg, to be less invasive on the overall lower extremity [26] and reduce risk of abandonment of the device [27]. A comparative analysis between passive and motorized knee exoskeleton is conducted. This paper focuses on developing the mathematical model for determining segmental moments and applying data obtained through biomechanical human modeling software of crouch gait to determine the effectiveness of a passive knee exoskeleton in the correction of four different crouch gaits.

2. Design and Methods

The process for design and simulation is summarized in Figure 2 wherein the exoskeleton was modelled to incorporate torsion springs in gait correction. Data was collected on all crouch gaits and the normal gait for purposes of a dynamic motion analysis followed by the sensitivity analysis and optimization of parameters to adjust the design as necessary.
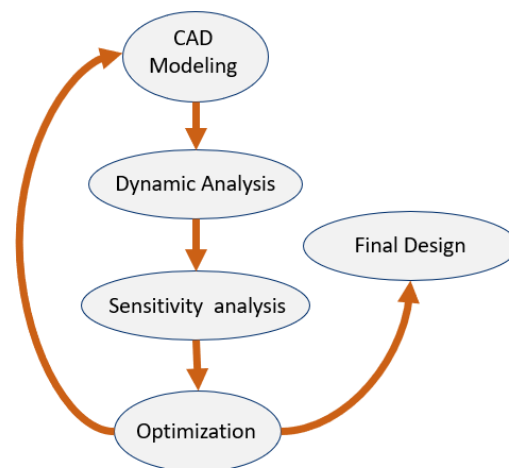

Figure 2. Schematic for overall process of exoskeleton design.

2.1. Mathematic model of human gait.

The equations of motion for the gait cycle were determined using the Euler-Lagrange method. The lower extremity was modelled as three hinged rigid rods. In the stance phase of the gait cycle the ground reaction forces (GRFs) are variable based on the weight of the subject, speed, type of gait, whereas the GRFs in the swing phase are zero for lack of contact with the ground. To account for this variability in the GRFs, Lagrange analyzes the

energy in the system. Since human gait is cyclical, it is assumed that energy in the system is conserved, thus Equation (1) was used to determine the angular accelerations for the hip, knee, and ankle joints.

$$\frac{d}{dt}\left(\frac{\partial \mathcal{L}}{\partial \dot{q}_i}\right) - \frac{\partial \mathcal{L}}{\partial q_i} = 0 \tag{1}$$

Where $\mathcal{L}$ represents the difference in kinetic and potential energies in the system with respect to the generalized velocities ($\dot{q}_i$), and displacements (q_i) for i variables in the system. The thigh, shank, and foot were modeled as three hinged rods at each respective joint as seen in Figure 3a.
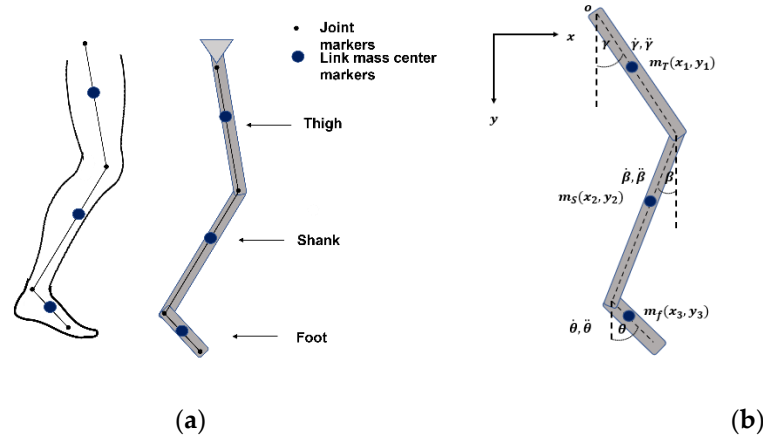

(a)   **(b)**

Figure 3. Figures for representation of (**a**) links, joints, and centers of mass for the leg segments and (**b**) corresponding free body diagram.

The three degree of freedom (DOF) model can be seen in Figure 3b with the origin at the top of the model, fixed to the upper body, wherein the motion for the upper body is considered negligible for the gait cycle. Translation and rotation are considered in the kinetic energies of the system with gravitational potential energy and converted to the generalized coordinates γ, β, θ, representing the angular displacements of the hip, knee, and ankle respectively. The resulting equations of motion are given in Equations (2-4), where the angular accelerations of the hip, knee, and ankle are represented by $\ddot{\gamma}, \ddot{\beta},$ and $\ddot{\theta}$, respectively.

$$\ddot{\gamma} = \frac{\left\{ \begin{array}{c} 0.443 m_S l_T l_S \left[\ddot{\beta}\cos(\gamma-\beta)-\dot{\beta}\sin(\gamma-\beta)(\dot{\gamma}-\dot{\beta})-\dot{\gamma}\dot{\beta}\sin(\gamma-\beta)\right]+m_f l_T l_S\left[\ddot{\beta}\cos(\gamma-\beta)-\dot{\beta}\sin(\gamma-\beta)(\dot{\gamma}-\dot{\beta})-\dot{\gamma}\dot{\beta}\sin(\gamma-\beta)\right] \\ + 0.436 m_f l_T l_f\left[\ddot{\theta}\sin(\gamma-\theta)(\dot{\gamma}-\dot{\theta})-\ddot{\theta}\cos(\gamma-\theta)+\dot{\gamma}\dot{\theta}\sin(\gamma-\theta)\right]+g l_T(m_T+m_S+m_f)\sin\gamma \end{array} \right\}}{l_T^2(0.9482 m_T+m_S+m_f)} \tag{2}$$

$$\ddot{\beta} = \frac{\left\{ \begin{array}{c} 0.443 m_S l_T l_S\left[\ddot{\gamma}\cos(\gamma-\beta)-\dot{\gamma}\sin(\gamma-\beta)(\dot{\gamma}-\dot{\beta})+\dot{\gamma}\dot{\beta}\sin(\gamma-\beta)\right]+m_f l_T l_S\left[\ddot{\gamma}\cos(\gamma-\beta)-\dot{\gamma}\sin(\gamma-\beta)(\dot{\gamma}-\dot{\beta})+\dot{\gamma}\dot{\beta}\sin(\gamma-\beta)\right] \\ +0.436\, m_f l_S l_f\left[\ddot{\theta}\cos(\beta-\theta)-\dot{\theta}\sin(\beta-\theta)(\dot{\beta}-\dot{\theta})+\dot{\beta}\dot{\theta}\sin(\beta-\theta)\right]+g l_S(m_S+m_f)\sin\beta \end{array} \right\}}{l_S^2(1.5295 m_S+m_f)} \tag{3}$$

$$\ddot{\theta} = \frac{\left\{ \begin{array}{c} 0.436 m_f l_S l_f\left[\ddot{\beta}\cos(\beta-\theta)-\dot{\beta}\sin(\beta-\theta)(\dot{\beta}-\dot{\theta})+\dot{\beta}\dot{\theta}\sin(\beta-\theta)\right]+0.436 m_f l_T l_f\left[\dot{\gamma}\sin(\gamma-\theta)(\dot{\gamma}-\dot{\theta})-\ddot{\gamma}\cos(\gamma-\theta)+\dot{\gamma}\dot{\theta}\sin(\gamma-\theta)\right] \\ + m_f g l_f \sin\theta \end{array} \right\}}{0.7133 m_f l_f^2} \tag{4}$$

The masses of each segment are represented as $m_T, m_S,$ and m_f, for the thigh, shank, and foot respectively. And the lengths for the thigh, shank, and foot are represented by $l_T, l_S,$ and l_f. For more details on derivation of the equations of motion, please see Appendix A. Since gait kinematics vary the masses and lengths are left as constants to be determined. Determining the mass moments of inertia in calculating the rotational kinematic energy, the centers of mass were determined by considering the proportional distance from the proximal joint for the right thigh, right shank, and right foot, as outlined in Table 1.

Table 1. Design parameters used to determine dimensions of wearable exoskeleton.

Segment	Circumference (cm)
Shank	39.5
Thigh	52.0

2.2. OpenSim 4.3: gait cyle simulation

OpenSim was used to show the two phases of the gait cycle. As seen in Figure 4 the gait cycle is separated by the weightbearing phase in the right leg for the first 60% of the gait cycle [7], followed the non-weightbearing swing phase, in the final 40%.
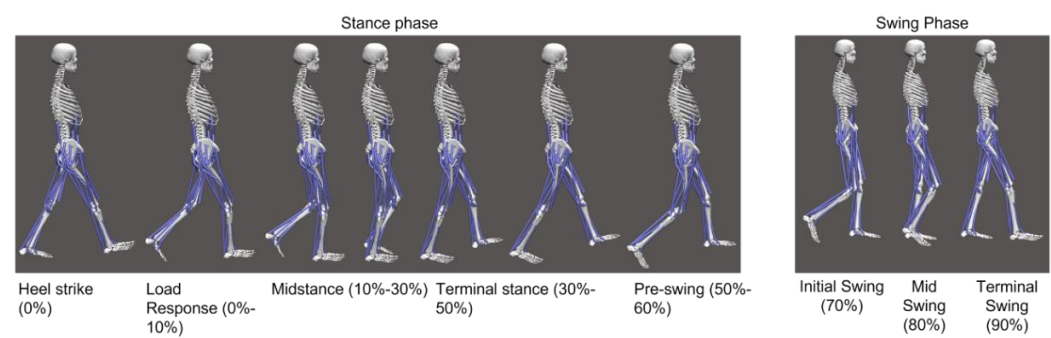

Figure 4. An OpenSim generated diagram for the stance and swing phase of the gait cycle.

Four versions of the crouch gait common in sufferers of cerebral palsy [2,4,5] were compared with that of a normal gait in OpenSim 4.3 to determine if the current model of the exoskeleton could potentially offload forces and stresses in the knee to aid in some non-invasive correction of the crouch gait. In this paper OpenSim 4.3 is used to establish parameters for testing the exoskeleton design. OpenSim is an opensource biomechanical software used to model human body dynamics that incorporates musculoskeletal systems for different segments of the human body. It comes with several preloaded models and motions, including a leg, arm, and an entire body for modeling gait.

2.2. SolidWorks: modeling and motion analysis

Two methods (passive only and passive with motorized knee angle correction) were used to determine the best options for offloading forces generated in the crouch gaits. The initial conditions were taken from the data obtained from OpenSim to determine the effectiveness of the current iterations by conducting a dynamic force analysis in SolidWorks and comparing it to the normal gait cycle. A motor was incorporated into the design and was used to control the knee angle. The first method used data points given from the angular rand of motion in the knees of each crouch gait from OpenSim that were extracted and converted to comma-separated value (CSV) files and uploaded into the function builder for the motor in SolidWorks as indicated in Figure 5. The function builder plotted displacement, velocity, acceleration and jerk for the exoskeleton given crouch gait and normal gait parameters. This was used to model the crouch gait behavior of the leg in conjunction with the exoskeleton. The tendon forces acting in the knee for each crouch gait were plotted and extracted as CSV files which were uploaded as force parameters to act on the exoskeleton through the gait cycle. The stiffness values for the torsion spring were adjusted to prevent extreme flexion on the knee in the crouch gait cycles. The second method motorizes the exoskeleton itself. Data points acquired from the angular range of motion for the knee of the normal gait were input into the motor, while importing data points for the tendon forces acting from the knee of the crouch gait.
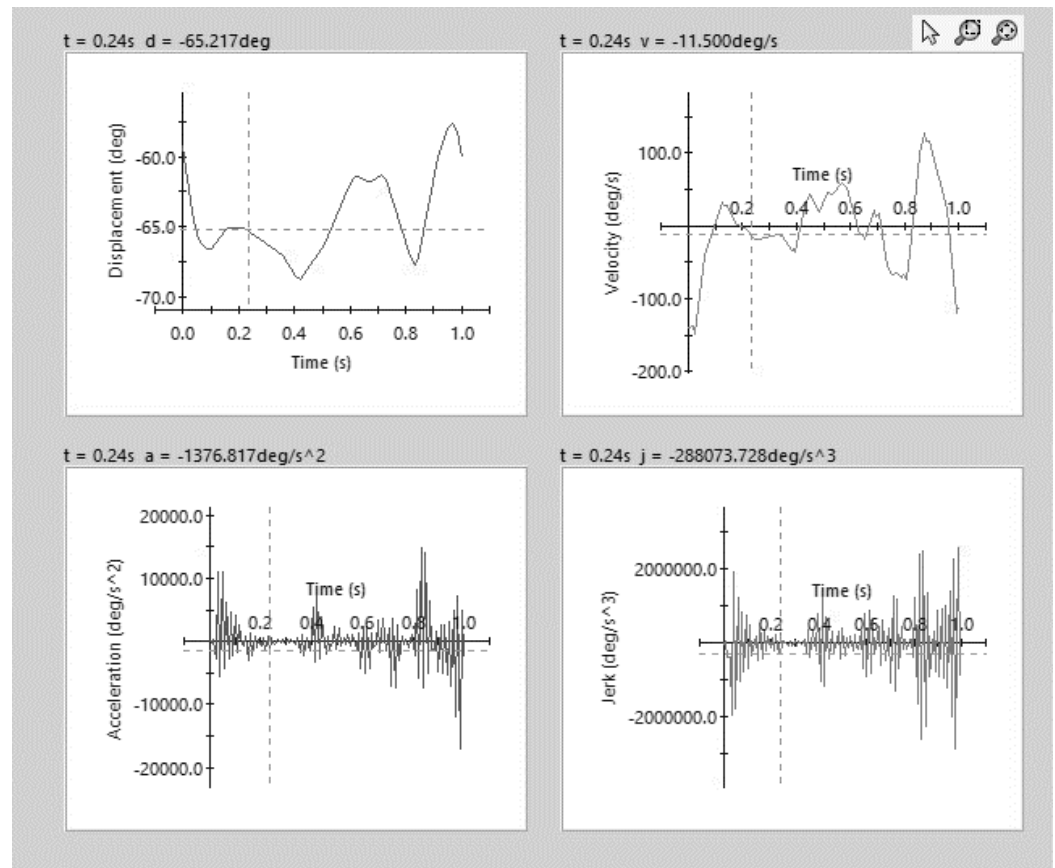
Figure 5. SolidWorks function builder used for angular displacement of the knee for crouch gait 1.

The first two iterations of the knee exoskeleton involve a frame that, when paired with lightweight fabric, the thigh support rests on the posterior side of the thigh, such that interference with the quadriceps is minimal as shown in Figures 6a and 6b. To limit over-flexion of the knee during the stance phase, torsional springs were used in the knee joint. Flexion of the ankle occurs during flexion of the knee. By reducing flexion of only the knee, the goal is to naturally reduce flexion of the ankle, however ankle and plantar dorsiflexion has not been addressed by any iteration of the exoskeleton. The parameters for design involved finding average circumferences for the thigh [28] and the calf, as seen in Table 1, to determine the best fit for the exoskeleton. In addition, adjustments were made to account for the incorporation of fabric for more comfort to the wearer. The first iteration was designed to solely be worn around the posterior of the leg. The second iteration was designed to support the back of the thigh, with the portion below the knee to be worn around the shin. Each iteration incorporates torsional springs to inhibit flexion of the knee.
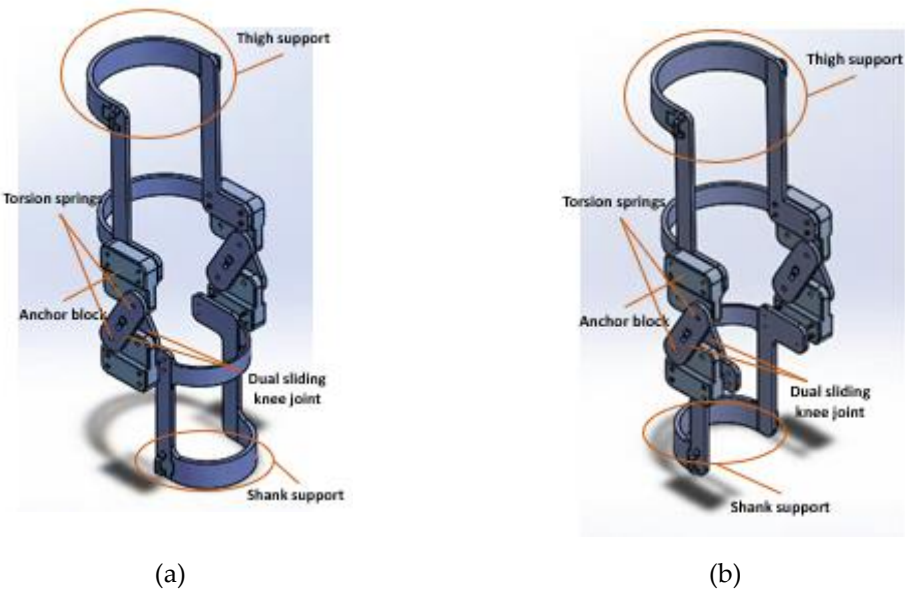
(a)   (b)

Figure 6. Two iterations of the passive exoskeleton where the thigh support should sit behind the thigh and (a) shank support is worn in front of the leg (b) shank support is worn behind the leg

After the determination of parameters in OpenSim to be used in the spring and motor components of the exoskeleton, placements had to be determined and the data points uploaded to SolidWorks. This process was used for both passive and motorized components of the exoskeleton. While motors were used in both, for the passive element the motor merely simulated the knee rotation of each crouch gait by a proportion of the gait cycle. In the motorized version of the exoskeleton, the motor serves as a corrective component by increasing the range of motion through the angles of the knee in the normal gait cycle. The final design, shown in Figure (9), incorporates through holes for straps to attach to the leg as well as additional springs to adjust for differing circumferences of the leg.
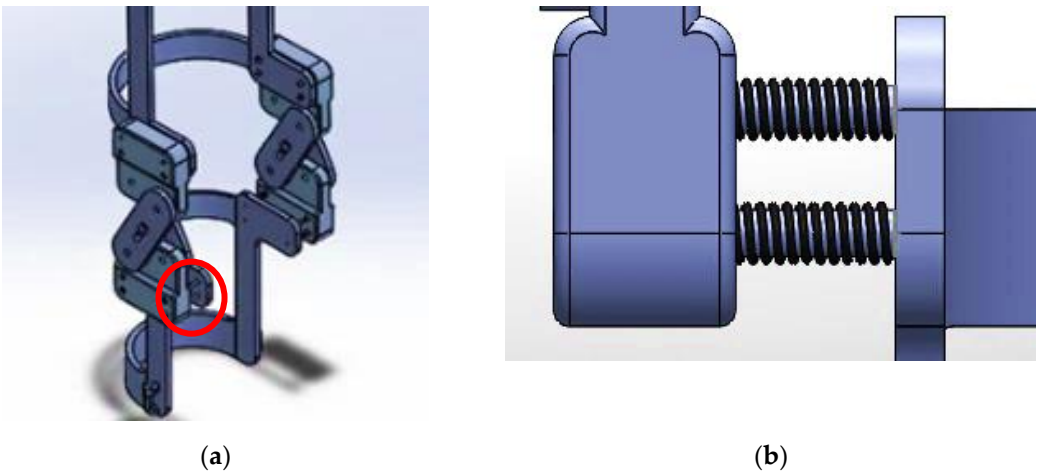

(a)   (b)

Figure 7. The final design of the exoskeleton (a) in its entirety and (b) a close up of the adjustable mechanism for leg circumference.

Figure 7a displays a comparison of the right knee moment produced throughout the gait cycle by plotting the sum of the moments for the muscles involved in knee extension,

including vastus intermedius, vastus lateralis, vastus medialis and rectus femoris. The green curve shows these moments for the normal gait. The blue curve is for the first crouch gait.   The orange curve represents the second crouch gait. The yellow curve represents the third crouch gait, while the purple curve represents the fourth crouch gait. Significant moments are produced and remain high or have limited range in crouch gaits 1 and 4 compared to that of the normal gait. Crouch gait 2 and 3 peak in the stance phase rather than the swing phase of the gait cycle.   They each begin with high moments compared to that of the normal gait as a result of ankle dorsiflexion in the stance phase. Additionally, as shown in Figure 8b forces generated in the knee during the stance phase are significantly higher in each of the crouch gaits compared to that of the normal gait.   These forces remain high in both phases of the gait cycle.
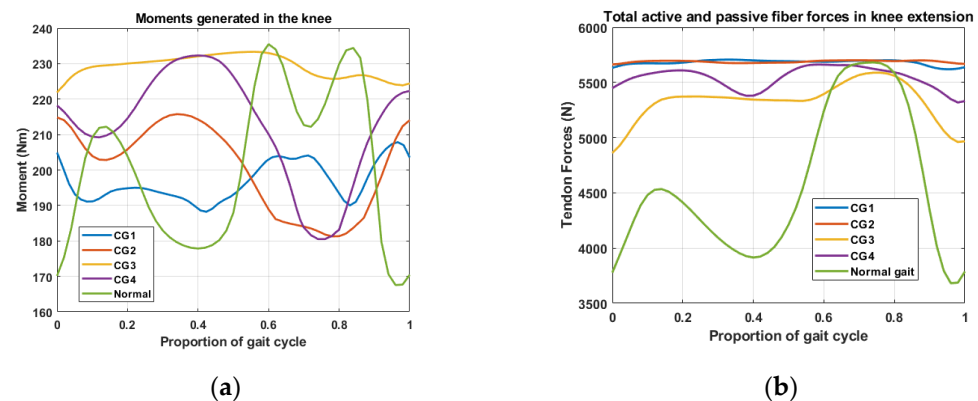

Figure 8. Graphs of (**a**) the moments generated in the knee throughout the gait cycle; (**b**) total active and passive fiber forces generated in the knee extensors.

3. Results

3.1. Passive correction (torsion spring only)

For the normal stance phase of the gait cycle, maxima and minima occur at 14% and 40%, respectively. As seen in Figure 9a, the maximum moment generated in the stance phase is 212194.5 Nmm and the minimum moment generated is 177,850.8 Nmm. The incorporation of torsion springs of 20k Nmm/deg showed an overall reduction in moments generated across all crouch gaits. CG2 (red curve) and CG 4 (purple curve) showed the greatest overall improvement in the stance phase of the gait cycle in terms of trend. CG2 maximum stance phase moment occurred at 12% at 118,782.2 Nmm while the minimum occurred at 36% at 106,115.8 Nmm. CG4 maximum stance phase moment occurred at 12% with 93,155.4 Nmm and the minimum occurs at 40% at 75,131.9.
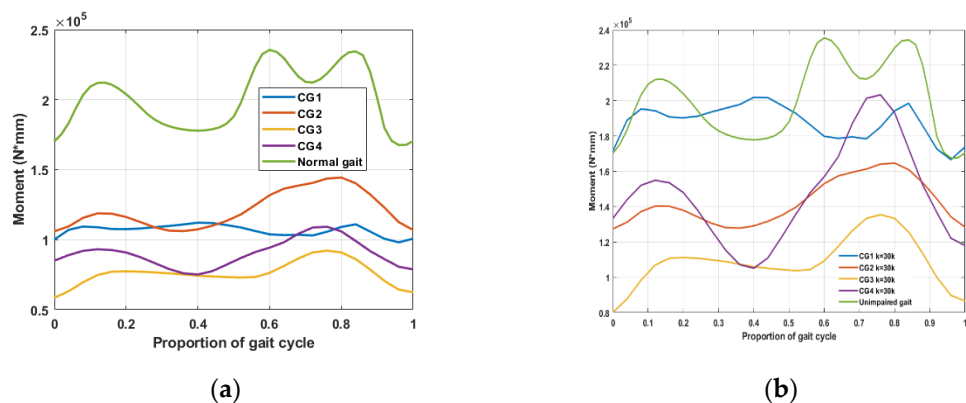

Figure 9. Graphs of the moments generated in the knee throughout the gait cycle using: (**a**) 20k Nmm/deg torsion springs and (**b**) 30k Nmm/deg torsion springs.

Torsion springs at 30k Nmm/deg significantly reduced moments in the stance phase in all crouch gaits except for CG 1 (blue curve) in Figure 9b. Peak moments trended toward the unimpaired (normal) gait curve in CG 2 (red curve) and CG 4 (purple curve). CG2 showed peak stance phase moments at 12% with 140,307.0 Nmm and 36% at 127,834.0. Peak moments in CG4 occurred at 12% at 154,915.8 Nmm and at 40% at 105,117.9 Nmm. All crouch gaits regardless of spring stiffness require improvement in the swing phase of the gait cycle. A significant adjustment of peak moments and their occurrences in the stance phase of the gait cycle across all gaits is noticeable with both the 20k Nmm/deg and 30k Nmm/deg torsion springs when compared to each uncorrected crouch gait.

3.2. Passive elements with motorized angular correction

Simulating a motor with the range of motion parameters for that of the normal knee angles, torsion springs of 20k Nmm/deg showed drastic drops in moments from the original crouch gaits. However, each crouch gait showed improvements in graphical trend with peak moments in the stance phase at 12% and minima at 40%. As seen in Figure 10a, maximum and minimum moments in CG2 (red curve) occurred at 51,730.6 Nmm and 42,701.4 Nmm, while CG 1 (blue curve) moments occurred at 51,566.5 Nmm and 42,931.9 Nmm and CG4 (purple curve) moments occurred at 51,238.6 Nmm and 40,5353.9 Nmm,
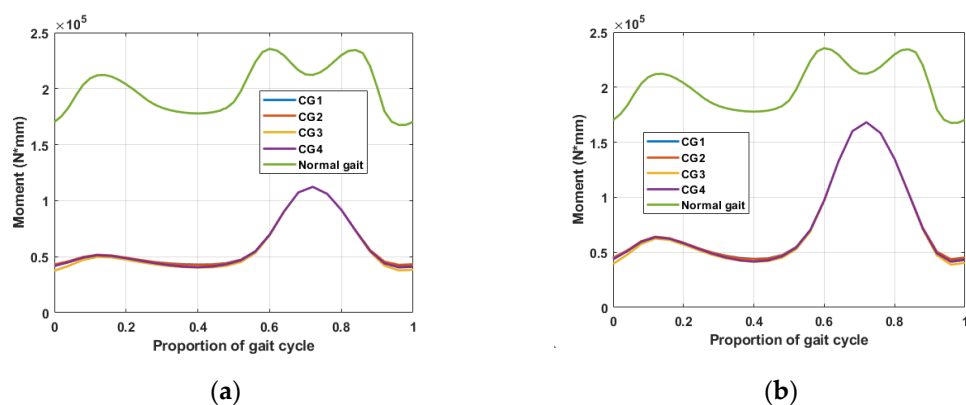

Figure 10. Graphs of passive elements with motorized angular knee correction using (**a**) 20k Nmm/deg torsion springs and (**b**) 30k Nmm/deg torsion springs.

Results using the 30k Nmm/deg torsions indicated further improvement in moment patterns generated in the stance phase across all CGs. Figure 10b displays moments generated with CG2 (red curve) peaks at 12% at 64,240.4 Nmm, while CG1 (blue curve) peaks at 12% at 64,088.1 Nmm. CG4 peaks at 12% in the gait cycle at 63,784.0 Nmm. At 40% of the gait cycle, the minimum for CG1 was 44,058.2 Nmm, CG2 was 43,828.5 Nmm, and CG 4 was 41,670.9 Nmm. All crouch gaits require improvement in the swing phase. Applying the combination of motorized components with the passive elements, a shift in moment trends occurs that more closely aligns with those of the normal gait cycle in the stance phase.

3.3. Gap analysis of the data

A summary of the data is found in Table 2 and 3. The noticeable differences between the human gait simulations and the simulations conducted in solid works are attributed to the physical differences between the simulations. All data was imported into Solid-Works from OpenSim. As such simulations were conducted with no segmental masses within the system. Moments generated are directly proportional to the angular accelerations and the mass moments of inertia. For purposes of creating motion within the exoskeleton the total fiber forces generated in knee extension were imported into SolidWorks

onto the device and in the direction of the forces at t=0. As such, the exoskeleton mass is very small when compared with the masses of each moving segment. This results in a lower mass moment of inertia with the exoskeleton segments, directly impacting the outcome of the moment generated in the exoskeleton simulation. It is expected that the moments generated when segmental masses and fiber forces are incorporated into an integrated simulation of the leg in conjunction with the exoskeleton, that the stance phase moments will increase toward that of the normal gait cycle.

Table 2. Moment maxima taken from simulations for each grouch gait.

Maximum moments	Torsion springs 20k Nmm/deg	%gait cycle	Motorized correction 20k Nmm/deg	%gait cycle	Torsion springs 30k Nmm/deg	%gait cycle	Motorized correction 30k Nmm/deg	%gait cycle
CG1	112117.5	40	51566.5	12	201854.6	60	64088.1	12
CG2	118782.2	12	51730.6	12	140307.0	12	64240.4	12
CG3	77376.4	20	49834.2	12	111187.3	20	62483.8	12
CG4	93155.36	12	51238.6	12	154915.8	12	63784.0	12

Table 3. Moment maxima taken from simulations for each grouch gait.

Minimum moments	Torsion springs 20k Nmm/deg	%gait cycle	Motorized correction 20k Nmm/deg	%gait cycle	Torsion springs 30k Nmm/deg	%gait cycle	Motorized correction 30k Nmm/deg	%gait cycle
CG1	103800.8	60	42931.9	40	179830.6	60	44058.2	40
CG2	106115.8	36	42701.4	40	127834	36	43828.5	40
CG3	72958.89	52	40303.2	40	103772.2	52	41439.1	40
CG4	75131.99	40	40535.92	40	105117.9	40	41670.9	40

Table 4. Moment maxima taken from simulations for each grouch gait.

Normal gait	Maximum moment	%gait cycle	Minimum Moment	%gait cycle
	212194.5	14	177850.8	40

4. Discussion

Different crouch gaits have been extensively difficult to define because of the various natures of causes. Crouch gaits may be caused in individuals with cerebral palsy which in and of itself has numerous subclassifications depending on the area of the brain impacted as well as how extensive hemiplegic, paraplegic or quadriplegic damage is done. Additional causes include traumatic brain injury, stroke, and other neurological problems as well as bone deformities. Correction may involve numerous treatment plans, including corrective orthotic devices and/or surgery. One problem with surgical treatment is that in many cases the outcome is unknown as to whether or not gait will improve [29]. One common surgical technique is lengthening of hamstrings, which may improve certain aspects of gait such as in the knee or ankle, however surgical treatment has the potential to cause additional problems [8].

Winters et al. helped define gait patterns in those with spastic hemiplegia that were placed into four separate groups. Comparisons with joints angles in the ankles, knees and hips and common symptoms differentiated between the groups. When comparing these graphs with the knee angles produced in each crouch gait produced in OpenSim, only crouch gait 3 and 4 contained similarities between two of the groups in Winters' assessments. In these cases, optimum improvement came with surgical procedures for lengthening the hamstrings. In many cases even after surgery, results of hamstring lengthening were inconsistent or did not work at all [14]. The incorporation of the torsional spring was able to counter excessive flexion moments produced in the [30] by applying the stored energy from knee flexion to provide necessary knee extension [31].

While these results are promising, torsion springs alone do not provide enough correction. With passive elements alone, the reduction in moment was one component of correction, however we saw that there needed to be a shift in the occurrence of peak moments. There was no improvement in CG 1 overall, while CG 3 still had peak moments occurring at 20% and 52%. CG 2 and CG 4 benefitted the most from the passive elements because peak moment occurrences at 12% for both and 36% and 40%, respectively, in the gait cycle. These gaits either did not change or were near that of the normal gait before and after motorized angular correction.

Since gait kinematics vary with different types of crouch gaits and source of crouch gait, it may be necessary to tailor torsion springs based on the individual needs of the subject and the severity of knee flexion. As seen in the results, a motorized component is necessary to aid in crouch gait rehabilitation. Ideally, incorporation of a lightweight, non-invasive, robotic element in knee angle correction, is advisable. This work is an incremental step in crouch gait correction in the stance phase. As such, we seek to address the swing phase in crouch gait as well as advancement in robotic elements of the knee exoskeleton.

5. Conclusions

The gait cycle is composed of two major phases; the stance phase and the swing phase, with subphases defined within each. The stance phase comprises 60% of the gait cycle while the swing phase comprises the final 40% of the gait cycle. Crouch gait is defined by excessive flexion of the knee during the stance phase of the gait cycle. Factors affecting crouch gait are numerous but are seen especially in those with cerebral palsy. Excessive flexion in the knee results in degradation of joints and mobility over time, resulting in complete loss of ambulation if left untreated. Exoskeletons for rehabilitative purposes are common for many such injuries and complications of the leg. While many exoskeletons are motorized for assistive mobility, it was sought to incorporate passive elements to reduce cost of the exoskeleton. Most exoskeletons are designed to be lower extremity worn, to correct ankle and hip rotation.

SolidWorks was used to model a lower limb exoskeleton to counter reaction forces produced in the knee for four different types of crouch gait. The exoskeleton was modelled using average circumferences for the thigh and shank and was modelled using passive elements to reduce the cost and to reduce invasiveness physiologically to keep the

exoskeleton lightweight. Most exoskeletons are designed to be lower-extremity worn to correct ankle and hip rotation.

SolidWorks was used to model a lower limb exoskeleton to counter reaction forces produced in the knee for four different types of crouch gait. The exoskeleton was modeled using average circumferences for the thigh and shank and was modeled using passive elements to reduce cost and to reduce invasiveness physiologically to keep the exoskeleton lightweight. Since ankle flexion is more pronounced during knee flexion, the team sought to explore the implications of the device for use solely on the knee. Torsional springs were incorporated to inhibit overflexion of the knee during the stance phase of the gait cycle. Dampers were included to reduce the recovery force of the spring entering the swing phase of the gait to prevent a forced overextension of the knee.

To establish parameters for testing the exoskeleton, OpenSim 4.3 was used. The angles of rotation during the gait cycle were plotted for four different crouch gaits and compared to the normal gait. Excessive forces, as well as moments, are produced in the knee because of excessive flexion during the stance phase of the gait cycle. The data points from forces and moments were exported as CSV files and applied to the exoskeleton, first incorporating only passive elements through the use of torsional springs while simulating the knee rotation of the four crouch gaits.

The gait cycle was set to 1s to analyze the proportion of the gait cycle in SolidWorks. Results from the passive elements indicated greatest improvements with both 20k Nmm/deg and 30k Nmm/deg in CG2 and CG4. The 30k Nmm/deg torsion spring simulations showed little to no improvement in CG1. The 30k Nmm/deg torsion springs showed greatest overall trend toward the normal gait, while the 20k Nmm torsion springs showed minor improvement over all crouch gaits, except for CG1 in the stance phase. The swing phase requires further improvement in all crouch gaits.

In the second round of testing, a motor was incorporated to drive the exoskeleton using the normal range of motion of the knee, while simulating forces on the exoskeleton from each crouch gait. All results showed the same trends as the normal knee angular displacement however using different spring stiffnesses resulted only in a change of magnitude of the moments generated. Thus, it was determined that best results would involve incorporating both passive and motorized elements while driving the exoskeleton using the normal range of motion in the knee for both angular and moment correction in crouch gait.

Appendix A

The derivations for the governing equations are as follows:

Position:

$$x_1 = 0.430 l_T \sin\gamma$$

$$x_2 = l_T \sin\gamma - 0.443 l_S \sin\beta$$

$$x_3 = l_T \sin\gamma - l_S \sin\beta + 0.436 l_f \sin\theta$$

$$y_1 = 0.430 l_T \cos\gamma$$

$$y_2 = l_T \cos\gamma + 0.443 l_S \cos\beta$$

$$y_3 = l_T \cos\gamma + l_S \cos\beta + 0.436 l_f \cos\theta$$

Velocity:

$$\dot{x}_1 = 0.430 \dot{\gamma} l_T \cos\gamma$$

$$\dot{x}_2 = \dot{\gamma} l_T \cos\gamma - 0.443 \dot{\beta} l_S \cos\beta$$

$$\dot{x}_3 = \dot{\gamma} l_T \cos\gamma - \dot{\beta} l_S \cos\beta + 0.436 \dot{\theta} l_f \cos\theta$$

$$\dot{y}_1 = -0.430 \dot{\gamma} l_T \sin\gamma$$

$$\dot{y}_2 = -\dot{\gamma} l_T \sin\gamma + 0.443 \dot{\beta} l_S \sin\beta$$

$$\dot{x}_3 = -\dot{\gamma} l_T \sin\gamma + \dot{\beta} l_S \sin\beta - 0.436 \dot{\theta} l_f \sin\theta$$

$$\mathcal{L} = T - V$$

Where T is the total translational and rotational energy in the system and V is the total potential energy in the system.

$$T = \sum \frac{1}{2} m_i (\dot{x}_i + \dot{y}_i)^2 + \sum \frac{1}{2} I \dot{\alpha}^2$$

Where α is used generally to represent the angular velocities of each segment.

$$I_0 = I_{segment} + m_i r^2$$

Where r is the distance from the proximal joint to the center of mass for each segment. After appropriate substitutions with generalized coordinates and trigonometric identities the total translational kenetic energy:

$$T_{1k} = 0.09245 m_T l_T^2 \gamma^2$$

$$T_{2k} = \frac{1}{2} m_S \left[\dot{\gamma}^2 l_T^2 + \dot{\beta}^2 l_S^2 - 0.886 \dot{\gamma} \dot{\beta} l_T l_S \cos(\gamma - \beta) \right]$$

$$T_{3k} = \frac{1}{2} m_f \left[\dot{\gamma}^2 l_T^2 + \dot{\beta}^2 l_S^2 + 0.190 \dot{\theta}^2 l_f^2 - 2 \dot{\gamma} \dot{\beta} l_T l_S \cos(\gamma - \beta) + 0.872 \dot{\gamma} \dot{\theta} l_T l_f \cos(\gamma - \theta) \right.$$
$$\left. - 0.872 \dot{\theta} \dot{\beta} l_S l_f \cos(\beta - \theta) \right]$$

The total rotational energy becomes:

$$T_{1r} = \frac{1}{6}\dot{\gamma}m_T l_T^2 + \frac{1}{2}\dot{\gamma}^2 m_T (0.430 l_T)^2$$

$$T_{2r} = \frac{1}{6}\dot{\beta}m_S l_S^2 + \frac{1}{2}\dot{\beta}^2 m_S (0.433 l_S)^2$$

$$T_{1r} = \frac{1}{6}\dot{\theta}m_f l_f^2 + \frac{1}{2}\dot{\theta}^2 m_f (0.436 l_f)^2$$

The constants to be squared are relative distances from the proximal joint to the center of mass.

The potential energy in the system is gravitational potential energy, thus:

$$V_1 = m_T g l_T \cos\gamma$$

$$V_2 = m_S g (l_T \cos\gamma + l_S \cos\beta)$$

$$V_3 = m_f g (l_T \cos\gamma + l_S \cos\beta + l_f \cos\theta)$$

The langrangian must be solved for each variable in the system to determine the governing equations.

$$\frac{d}{dt}\left(\frac{\partial T}{\partial \dot{\gamma}}\right) = \frac{\partial T}{\partial \gamma} - \frac{\partial V}{\partial \gamma}$$

$$\frac{d}{dt}\left(\frac{\partial T}{\partial \dot{\beta}}\right) = \frac{\partial T}{\partial \beta} - \frac{\partial V}{\partial \beta}$$

$$\frac{d}{dt}\left(\frac{\partial T}{\partial \dot{\theta}}\right) = \frac{\partial T}{\partial \theta} - \frac{\partial V}{\partial \theta}$$

References

1. Delp S.,L., Arnold A.,S., Piazza S.,J. Graphics-based modeling and analysis of gait abnormalities. *Biomedical Materials and Engineering*, **1998**, 8:227–240.
2. Steele K.,M., DeMers M.,S., Schwartz M.,H., Delp S.,L. Compressive tibiofemoral force during crouch gait. *Gait & posture*, **2012** 35(4):556–560.
3. Steele K.,M., van der Krogt M.,M., Schwartz M.,H., Delp S.,L. How much muscle strength is required to walk in a crouch gait? *Journal of biomechanics*, **2012** 45(15):2564–2569.
4. Lerner Z.,F., Damiano D.,L., Bulea T.,C. A robotic exoskeleton to treat crouch gait from cerebral palsy: Initial kinematic and neuromuscular evaluation. In 2016 38th Annual International Conference of the IEEE Engineering in Medicine and Biology Society (EMBC), pages 2214–2217. IEEE, 2016.
5. Ganjwala D., Shah H. Management of the knee problems in spastic cerebral palsy. *Indian journal of orthopaedics*, **2019,** 53(1):53–62.
6. Hilberink S.,R., Roebroeck M.,E., Nieuwstraten W., Jalink L., Verheijden J., Stam H.,J. Health issues in young adults with cerebral palsy: towards a life-span perspective. 2007.
7. Shah K., Solan M., Dawe E.. The gait cycle and its variations with disease and injury. *Orthopaedics and Trauma*, **2020,** 34(3):153–160.
8. Arnold A.,S., Liu M.,Q., Schwartz M.,H., Ounpuu S., Delp S.,L. The role of estimating muscle-tendon lengths and velocities of the hamstrings in the evaluation and treatment of crouch gait. *Gait & posture*, **2006,** 23(3):273–281.
9. Rose J., Gamble J.G., Medeiros J., Burgos A., Haskell W.L. Energy cost of walking in normal children and in those with cerebral palsy: comparison of heart rate and oxygen uptake. *J Pediatr Orthop*, **1989,** 9(3):276–279.
10. Waters R.L., Mulroy S. The energy expenditure of normal and pathologic gait. *Gait & posture*, **1999,** 9(3):207–231.
11. Jahnsen R., Villien L., Aamodt G., Stanghelle J., Holm I. Musculoskeletal pain in adults with cerebral palsy compared with the general population. *Journal of Rehabilitation Medicine*, **2004**, 36(2):78–84.
12. Bottos M., Gericke C. Ambulatory capacity in cerebral palsy: prognostic criteria and consequences for intervention. *Developmental medicine and child neurology*, **2003**, 45(11):786–790.
13. Brandon S.,C., Thelen D.,G., Smith C.,R., Novacheck T.,F., Schwartz M.,H., Lenhart R.,L. The coupled effects of crouch gait and patella alta on tibiofemoral and patellofemoral cartilage loading in children. *Gait & posture*, **2018,** 60:181–187.

14. Park H., Park B.,K., Park K.,B., Abdel-Baki S.,W., Rhee I., Kim C.,W., Kim H.,W. Distal femoral shortening osteotomy for severe knee flexion contracture and crouch gait in cerebral palsy. *Journal of clinical medicine*, **2019,** 8(9):1354.

15. Pelrine E.,R., Novacheck T.,F., Boyer E.,R. Knee pain and crouch gait in individuals with cerebral palsy: what impact does crouch-related surgery have? *Developmental Medicine & Child Neurology*, **2020** 62(6):709–713.

16. Graham H.,K., Selber P. Musculoskeletal aspects of cerebral palsy. *The Journal of bone and joint surgery British volume*, **2003,** 85(2):157–166.

17. Mullaji A., Shetty G.,M. Persistent hindfoot valgus causes lateral deviation of weightbearing axis after total knee arthroplasty. *Clinical Orthopaedics and Related Research®*, **2011,** 469(4):1154–1160.

18. Patthanacharoenphon C., Maples D.,L., Saad C., Forness M.,J., Halanski M.,A. The effects of patellar tendon advancement on the immature proximal tibia. *Journal of children's orthopaedics*, **2013,** 7(2):139–146.

19. Li G., DeFrate L., Zayontz S., Park S., Gill T. The effect of tibiofemoral joint kinematics on patellofemoral contact pressures under simulated muscle loads. *Journal of orthopaedic research*, **2004,** 22(4):801–806.

20. Classification of Gait Patterns in Cerebral Palsy. (2019, September 13). Physiopedia, Retrieved 21:56, November 29, 2021 from https://www.physio-pedia.com/index.php?title=Classification_of_Gait_Patterns_in_Cerebral_Palsy&oldid=222810.

21. Bregman D.,J., Van der Krogt M., De Groot V., Harlaar J., Wisse M., Collins S. The effect of ankle foot orthosis stiffness on the energy cost of walking: a simulation study. *Clinical Biomechanics*, **2011,** 26(9):955–961.

22. Kerkum Y.,L., Buizer A.,I., Van Den Noort J.,C., Becher J.,G., Harlaar J., Brehm M.,A. The effects of varying ankle foot orthosis stiffness on gait in children with spastic cerebral palsy who walk with excessive knee flexion. *PloS one*, **2015,** 10(11):e0142878.

23. Damiano D.,L., Arnold A.,S., Steele K.,M., Delp S.,L. Can strength training predictably improve gait kinematics? a pilot study on the effects of hip and knee extensor strengthening on lower-extremity alignment in cerebral palsy. *Physical therapy*, **2010,** 90(2):269–279.

24. Collins S.,H., Wiggin M.,B., Sawicki G.,S. Reducing the energy cost of human walking using an unpowered exoskeleton. *Nature,* **2015,** 522(7555):212–215.

25. Naf M.,B., Junius K., Rossini M., Rodriguez-Guerrero C., Vanderborght B., Lefeber D. Misalignment compensation for full human-exoskeleton kinematic compatibility: state of the art and evaluation. *Applied Mechanics Reviews*, **2018,** 70(5).

26. Scherer, M.J., 1996, "Outcomes of Assistive Technology Use on Quality of Life," Disability Rehabil., 18(9), pp. 439–448.

27. Jung KJ, Kimm H, Yun JE, Jee SH. Thigh circumference and diabetes: obesity as a potential effect modifier. *Journal of epidemiology*, **2013,** 23(5):329–336.

28. Hicks J.,L., Delp S.,L., Schwartz M.,H. Can biomechanical variables predict improvement in crouch gait? *Gait & posture,* **2011,** 34(2):197–201.

29. Chaichaowarat R., Granados D.,F.,P., Kinugawa J., Kosuge K. Passive knee exoskeleton using torsion spring for cycling assistance. In 2017 IEEE/RSJ International Conference on Intelligent Robots and Systems (IROS), pages 3069–3074. IEEE, 2017.

30. Spring AN, Kofman J, Lemaire ED. Design and evaluation of an orthotic knee-extension assist. IEEE Transactions on Neural Systems and Rehabilitation Engineering, **2012,** 20(5):678–687.

31. Winters, T.F., Gage, J.R. and Hicks, R. Gait patterns in spastic hemiplegia in children and young adults. *J Bone Joint Surg Am*, **1987,** *69*(3), pp.437-441.